I wish to acknowledge the financial support given to this work by the Australian Nuclear Science and Technology Organisation under Research Contract No. 82/X/1. The neutron powder data for this work were collected at the Insitut Laue–Langevin, Grenoble, and I am indebted in particular to Dr Alan Hewat for providing access to the excellent facilities at this laboratory. Many thanks are extended to Joanne Hodge for assistance with the sample preparation.

References

BLACKMAN, M. (1956). *Acta Cryst.* **9**, 734–737.
BURSILL, L. A. & GRZINIC, G. (1980). *Acta Cryst.* B**36**, 2902–2913.
CHEARY, R. W. (1986). *Acta Cryst.* B**42**, 229–236.
CHEARY, R. W. (1987). *Acta Cryst.* B**43**, 28–34.
CHEARY, R. W. (1988). *Mater. Sci. Forum*, **27**, 397–406.
CHEARY, R. W. (1990). *Acta Cryst.* B**46**, 599–609.
CHEARY, R. W. & SQUADRITO, R. (1989). *Acta Cryst.* B**45**, 205–212.
FIELDING, P. E. & WHITE, T. J. (1987). *J. Mater. Res.* **2**, 387–414.
HEWAT, A. (1979). *Acta Cryst.* A**35**, 248.
HEWAT, A. (1986). *Mater. Sci. Forum*, **9**, 69–80.
HOUSLEY, H. M. & HESS, F. (1966). *Phys. Rev.* **146**, 517–526.
HOWARD, C. J. (1982). *J. Appl. Cryst.* **15**, 615–620.
HOWARD, C. J. & HILL, R. J. (1986). Report AAEC/M112. Australian Atomic Energy Commission, Lucas Heights Research Laboratories, Australia.
KESSON, S. E. & WHITE, T. J. (1986*a*). *Proc. R. Soc. London Ser. A*, **405**, 73–101.
KESSON, S. E. & WHITE, T. J. (1986*b*). *Proc. R. Soc. London Ser. A*, **408**, 295–319.
POST, J. E., VON DREELE, R. B. & BUSECK, P. R. (1982). *Acta Cryst.* B**38**, 1056–1065.
ROTH, R. (1981). Annual Report NBSIR81-2241. National Measurements Laboratory, Office of Nuclear Technology, Australia.
SABINE, T. M. & HEWAT, A. (1982). *J. Nucl. Mater.* **110**, 173–177.
SHANNON, R. D. (1976). *Acta Cryst.* A**32**, 751–767.
WILES, D. B. & YOUNG, R. A. (1981). *J. Appl. Cryst.* **14**, 149–150.

Acta Cryst. (1991). B**47**, 333–337

The Commensurate (10/4) Cluster Model in Quenched Wüstite P''. New Simulation of HREM Direct Images

BY G. NIHOUL

GMET, Université de Toulon et du Var, BP 132, 83957 *La Garde CEDEX, France*

J.-R. GAVARRI

LCMPCT, Université de Toulon et du Var, 83957 *La Garde CEDEX, France*

AND C. CAREL

Laboratoire de Cristallochimie, Université de Rennes I, 35042 *Rennes CEDEX, France*

(*Received* 24 *May* 1990; *accepted* 6 *December* 1990)

Abstract

In the case of non-stoichiometric quenched wüstite P'' with the formula $Fe_{1-z}O$ ($z \simeq 0{\cdot}096$), the defect structure is shown to consist most probably of clusters composed of ten vacancies and four interstitial Fe^{III} ions. These clusters are in agreement with a long-range ordering ($2{\cdot}5X$, $2{\cdot}5X$, $5X$), with some disorder in their local arrangement. The direct images of the quenched phase P'', previously obtained by various authors, are reinterpreted from a (10/4) cluster model: computer simulations have been carried out using this new model. The simulated images are in good agreement with the experimental images found in the literature.

I. Introduction

In the Fe–O system, iron monoxide or wüstite shows a particularly large deviation from stoichiometry and a complex behavior under equilibrium conditions at high temperature (Vallet & Carel, 1989). This is why many previous structural studies (Koch & Cohen, 1969; Cheetham, Fender & Taylor, 1971; Catlow & Fender, 1975; Gavarri, Carel & Weigel, 1979; Gavarri, Carel, Jasienska & Janowski, 1981; Gartstein, Mason & Cohen, 1986) have been performed on this material at high temperature or after quenching. It has been shown that the wüstites are characterized by various types of clustering of vacancies (□) and interstitial Fe^{III} ions occupying the octahedral (octa) and tetrahedral (tetra) sites respectively of the NaCl lattice with the general formula:

$$Fe_{1-z}O \equiv [Fe^{2+}]^{octa}_{1-3z}[Fe^{3+}]^{octa}_{2z-t}[Fe^{3+}]^{tetra}_{t}[\square]_{z+t}O^{2-}$$

In more recent studies (Gavarri *et al.*, 1979, Gartstein *et al.*, 1986; Gavarri & Carel, 1989; Carel & Gavarri, 1990), the ratio $R = (z + t)/t$ has been shown to be close to $2{\cdot}4 \pm 0{\cdot}4$ for quenched and

0108-7681/91/030333-05$03.00

high-temperature samples. Such a value suggested the possible presence of clusters made up of ten vacancies (□) and four interstitial Fe^{III} ions with a zinc blende type structure as described in Fig. 1(*a*). However, several other interpretations are possible because of insufficient information provided by the powder diffraction data (Gavarri *et al.*, 1979).

The long-range ordering of these clusters of defects in quenched wüstites can now be reexamined taking new experimental and theoretical work into account:

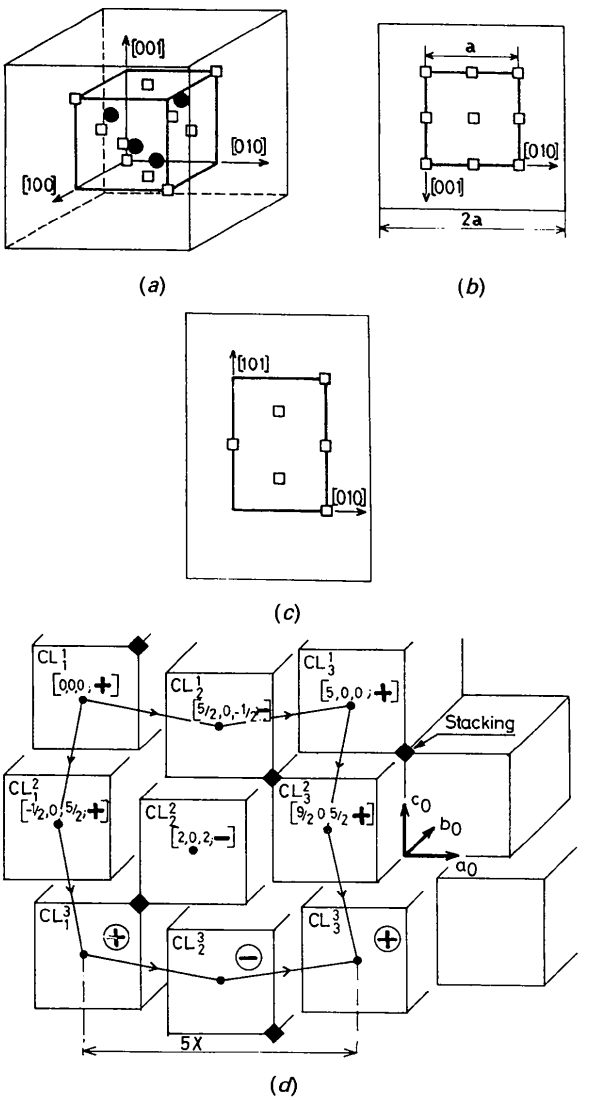

Fig. 1. (*a*) The (10/4) cluster with its envelope: the Fe^{III} tetrahedral sites are represented by black circles, the octahedral vacancies by empty squares. The cube dimension is $2a_0$. (*b*) [100] projection of the vacancies and envelope. (*c*) [110] projection of the vacancies and envelope: note the distribution of vacancy projected lines. (*d*) Stacking of clusters with their envelope. Only one layer is represented [plane (010)]. The existence of zigzags is determined by the NaCl type lattice and connected with the cluster orientation (+) or (−). The pairs of clusters are marked with their common edges. Stacking faults can be represented.

(*a*) Several electron diffraction patterns (Lebreton & Hobbs, 1983) and high-resolution electron microscopy (HREM) images (Iijima, 1974; Ishiguro & Nagakura, 1985, 1986) have given clear evidence of defect clustering, probably with a local tetragonal or cubic apparent symmetry.

(*b*) Generally, it has been shown that the long-range ordering is not cubic; a ($2{\cdot}5X$, $2{\cdot}5X$, $5X$) superstructure has frequently been observed linked with the presence of stacking faults for values of z close to 0·09–0·10 (Andersson & Sletnes, 1977; Ishiguro & Nagakura, 1985, 1986).

(*c*) From a recent energy model, the higher stability of such (10/4) clusters has been justified (Gavarri & Carel, 1989; Carel & Gavarri, 1990) and used for interpreting the structural evolution of substituted wüstites after Andersson, Grimes & Heuer (1984) who have emphasized this cluster amongst several others.

(*d*) In the HREM study carried out by Ishiguro & Nagakura (1985, 1986), the direct images of wüstite P'' were interpreted in terms of a local $5X$ superstructure of small elongated clusters consisting of six vacancies, with stacking faults and domains. On the direct images obtained in the [001] direction, characteristic rods were interpreted in terms of vertical superimposed (6/0) or (6/2) clusters forming layers. On the direct images obtained in the [101] direction, alternate rhombs and distorted centered rectangles were observed. From their electron diffraction patterns, these authors interpreted the reciprocal space in terms of space group $P2_1/m$, consistent with the new superstructure cell based on the periodicities ($2{\cdot}5X$, $2{\cdot}5X$, $5X$).

We present here a new interpretation of the HREM images obtained by Ishiguro & Nagakura (1985, 1986) based on the (10/4) cluster model previously proposed (Andersson *et al.*, 1984). We first recall the model, then compute images obtained from this model in a high-resolution electron microscope.

II. The (10/4) cluster model and the superstructure ($2{\cdot}5X$, $2{\cdot}5X$, $5X$)

This wüstite model has an elemental (10/4) cluster with the zinc blende structure (Andersson *et al.*, 1984). Figs. 1(*a–c*) show an extended cubic cluster (Gavarri, Carel & Weigel, 1988) made up of a (10/4) cluster and a stoichiometric cubic envelope, where eight Fe^{3+} ions are assumed to be localized in octahedral sites. The envelope parameter is $2a_0$ where a_0 is the mean cubic cell parameter of the wüstite. Each extended cluster is denoted $CL_j^i[x, y, z:\pm]$, where i and j are the number of the layer and the number locating the cluster inside the layer respectively; x, y and z are the coordinates of the cluster center. The negative clusters are obtained from the positive ones *via* a 90° rotation about the [100] axis.

Clusters CL_j^i are arranged alternately in the (001) plane at intervals given by vectors $5/2\mathbf{a_0} \pm 1/2\mathbf{b_0}$ and $5/2\mathbf{b_0} \pm 1/2\mathbf{a_0}$. This arrangement requires a cluster layer (010). In this layer, two extended clusters share one edge forming twin cube blocks. Each block is oriented perpendicularly with regard to surrounding blocks in the same layer. In the [001] direction, the clusters are translated alternatively by vectors $5/2\mathbf{c_0} \pm 1/2\mathbf{b_0}$. Such a (010) layer of clusters CL_j^i is represented in Fig. 1(*d*).

Under these conditions, the space group is $P11a$ with eight clusters (10/4) per supercell. This corresponds to a departure from the stoichiometry by $z = 48/500 = 0{\cdot}096$. A stacking fault, such as represented on the figure, is in agreement with the selection rules observed on the electron diffraction patterns of Ishiguro & Nagakura (1985, 1986).

Projections onto the (100) and (101) planes are shown on Figs. 2(*a*) and 2(*b*): only the vacancies and interstitial Fe^{3+} ions are indicated. One can see that the [100] projected vacancies are aligned, while the [101] dense axis vacancies show alternate lines and rhombs.

III. Interpretation of HREM images from the (10/4) cluster model

The high-resolution electron microscopy study carried out by Ishiguro & Nagakura (1985, 1986) shows images of wüstite P'' phase obtained in a 1 MeV microscope (corresponding wavelength $l = 0{\cdot}87$ pm

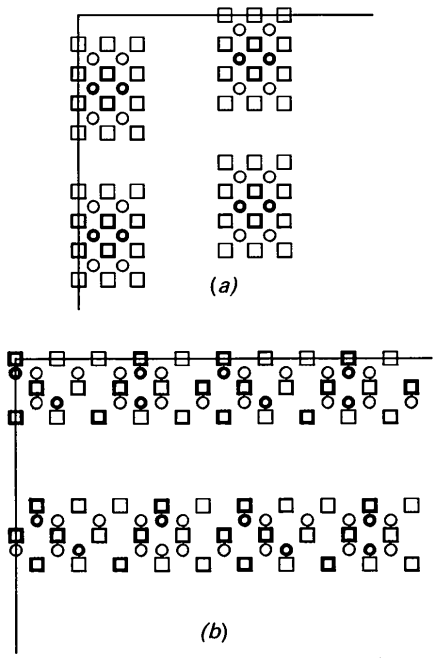

Fig. 2. Projection of the superlattice on the (100) plane (*a*) and the (110) plane (*b*). Only the vacancies (□) and the interstitial (○) Fe^{3+} ions have been shown.

Table 1. *Projected cells derived from the superstructure cell*

	[100]	[110]
Projected cell (Å)		
-A-	21·5	21·5
-B-	21·5	30·1
g_{limit} (Å^{-1})	5·9	4·2

$= 0{\cdot}0087$ Å). The operating parameters of the microscope were: spherical-aberration coefficient $C_s = 2{\cdot}5$ mm, chromatic defocus spread 20 nm and beam divergence 4×10^{-4} rad; no objective aperture was used.

The interpretation of HREM images can only be carried out by computing images from a model, including in the calculations the passage of the electrons through the modelled crystal and the transfer of the outgoing wave through the microscope, taking into account the defocus and aberrations of the objective lens and the divergence of the incident wave. The authors of the HREM study mentioned above have calculated images from their model [clusters (6/0) or (6/2) arranged in a monoclinic pseudotetragonal way]. Although there is some similarity between their computed images and the experimental ones, it cannot be said that the agreement is satisfactory.

We have computed images using the model described in the previous paragraphs. The passage of electrons through the crystal is described using the multislice method (see Cowley, 1975). The superstructure cell ($5X$, $5X$) is projected along the [100] and [110] directions giving the projected cells shown in Table 1. The sampling is based on 256 points along A and B, which means that the distance between two sampling points is equal to or lower than 0·1 Å. The projected potential is calculated from structure factors corresponding to spatial frequencies lower than the g_{limit} shown in Table 1. Finally, a Debye–Waller correction is included in the calculations. The transfer of the electronic outcoming wave through the microscope is described in the customary way, using the same parameters as those employed by Ishiguro & Nagakura (1985, 1986).

Fig. 3 shows the images computed for an observation along the [100] axis and for several defocuses. The wüstite crystal thicknesses are 45 Å (*a* to *d*) and 60 Å (*e* to *h*). Images (*a*) and (*e*) corresponding to a defocus of -900 Å agree very well with the experimental images published by Ishiguro & Nagakura (1985, 1986). The white dots have unequal brightness and one can clearly see two groups of three very bright dots bordered by two groups of three medium dots, the remaining white dots being pale. Let us recall that these dots represent atomic rows parallel to the observation direction (*i.e.* [100]) and are composed of Fe and O atoms. Furthermore, we can

observe that the bordering and surrounding spots get brighter as the thickness increases. On the experimental image, there is an obvious change of contrast from one part of the image to the other showing a slight change in thickness. It is very seldom that flakes have exactly parallel surfaces: they more often have a wedge shape. In the present case, the upper part of the image would correspond to a thickness of 45 Å while the lower part would be 60 Å thick. Let us recall that the authors estimated the defocus as −900 Å and the thickness as 60 Å from other measurements. Consequently we can say that the new model proposed here for the clustering and its ordering agrees very closely with the HREM image obtained along the [100] axis by Ishiguro & Nagakura (1985, 1986).

Fig. 4 shows images computed for an observation along the [110] axis. Defocuses vary from −1200 to

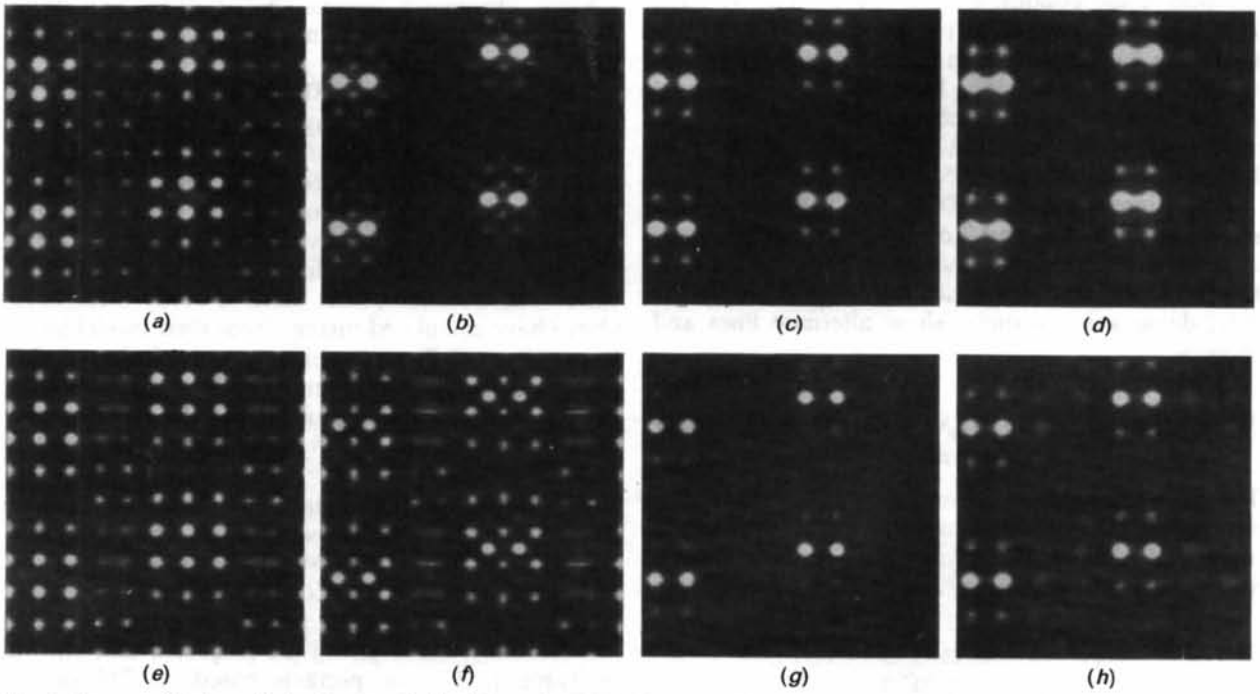

Fig. 3. Computed high-resolution images obtained from the (10/4) cluster model, observed along the [100] axis. Crystal thicknesses are 45 (*a* to *d*) and 60 Å (*e* to *h*). The defocuses are − 900 (*a*, *e*), −825 (*b*, *f*), −750 (*c*, *g*) and −675 Å (*d*, *h*).

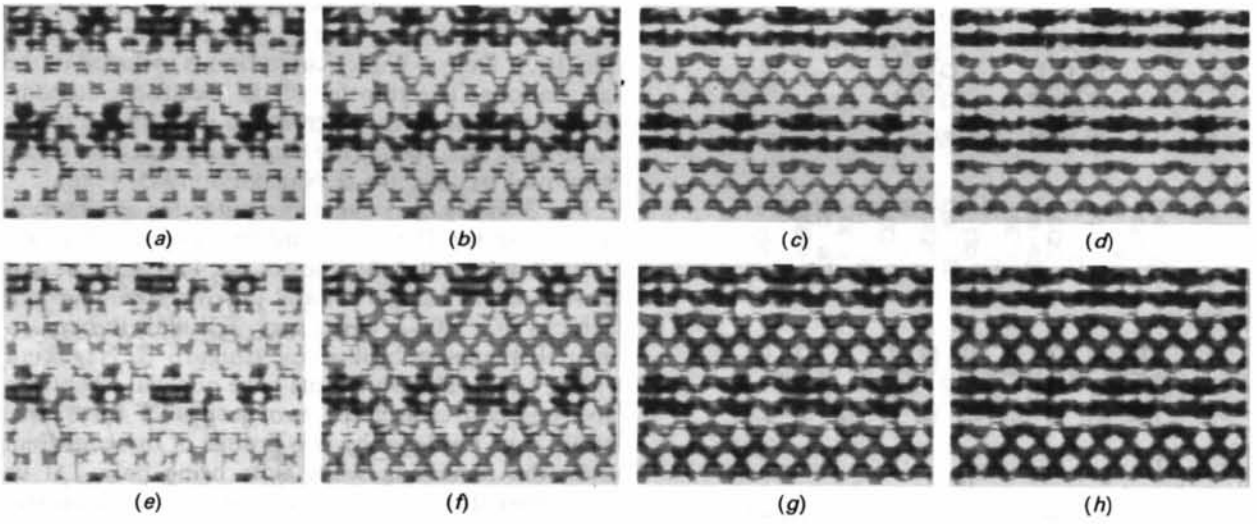

Fig. 4. Computed high-resolution images obtained from the (10/4) cluster model observed along the [110] axis. Crystal thicknesses are 100 (*a* to *d*) and 115 Å (*e* to *h*). Defocuses are − 120 (*a*, *e*), −1100 (*b*, *f*), −1000 (*c*, *g*) and −900 Å (*d*, *h*).

−900 Å and wüstite thicknesses are 100 and 115 Å. The model used here is an ordered one with all vacancies placed in the same locations for the whole of the crystal. One can see figures similar to those obtained on the [110] projection by Ishiguro & Nagakura (1985, 1986).

IV. Discussion and concluding remarks

For the images obtained with an electron beam parallel to the [100] axis, there is no doubt that the images computed with the (10/4) cluster model fit the experimental image obtained by Ishiguro & Nagakura (1985, 1986) much better than the images computed by them with a (6/0) or (6/2) cluster model. We can even explain the variation of contrast observed in the image by a slight change in the wüstite flake thickness.

When the electron beam is parallel to the [110] axis, a difference appears between our computed images and the experimental HREM image. However, this is easily explained by the existence of some disorder concerning the stacking of the negative and positive clusters (remember that one cluster is obtained from the other by a 90° rotation about the [100] axis) because there is no reason why there should only be positive clusters stacked on top of each other. In addition, stacking faults can be clearly observed in the [100] direct images of Ishiguro & Nagakura (1985, 1986). If one postulates the existence of disorder in the stacking, the rhombs remain rhombs, but the dense lines become centered rectangles, in which case the experimental HREM images are quite well fitted.

In this study, we have shown that simulated images of the defect structure of quenched wüstite P'', based on layers of (10/4) clusters, is consistent with the observed HREM direct images obtained by Ishiguro & Nagakura (1985, 1986) and Iijima (1974). This consistency leads to an understanding of a great number of converging structural observations found in the literature, especially the value of the ratio $R = (z + t)/t = 2{\cdot}4$ found in a new set of neutron diffraction experiments (Gavarri, Jasienska, Orewczyk & Janowski, 1987; Carel & Gavarri, 1990).

References

ANDERSSON, A. B., GRIMES, R. W. & HEUER, A. H. (1984). *J. Solid State Chem.* **55**, 353–361.

ANDERSSON, A. B. & SLETNES, J. O. (1977). *Acta Cryst.* A**33**, 268–276.

CAREL, C. & GAVARRI, J.-R. (1990). *J. Phys. Chem. Solids*, **51**, 1131–1136.

CATLOW, C. R. A. & FENDER, B. E. F. (1975). *J. Phys. C*, **8**, 3267–3279.

CHEETHAM, A. K., FENDER, B. E. F. & TAYLOR, R. I. (1971). *J. Phys. C*, **4**, 2160–2165.

COWLEY, J. M. (1975). *Diffraction Physics*. Amsterdam: North Holland.

GARTSTEIN, E. Z., MASON, T. O. & COHEN, J. B. (1986). *J. Phys. Chem. Solids*, **47**, 759–773, 775–781.

GAVARRI, J.-R. & CAREL, C. (1989). *Phase Transit.* **14**, 103–108.

GAVARRI, J.-R., CAREL, C., JASIENSKA, ST. & JANOWSKI, J. (1981). *Rev. Chim. Miner.* **18**, 608–624.

GAVARRI, J.-R., CAREL, C. & WEIGEL, D. (1979). *J. Solid State Chem.* **29**, 81–95.

GAVARRI, J.-R., CAREL, C. & WEIGEL, D. (1988). *C. R. Acad. Sci.* **307**(II), 705–711.

GAVARRI, J.-R., JASIENSKA, ST., OREWCZYK, J. & JANOWSKI, J. (1987). *Metal. Odlew. Krakow*, **13**, 1–2, 43–62.

IIJIMA, S. (1974). *Electron Microsc. Soc. Am.* **32**, 352–353.

ISHIGURO, T. & NAGAKURA, S. (1985). *Jpn. J. Appl. Phys.* **24**, L723–L726.

ISHIGURO, T. & NAGAKURA, S. (1986). Proc. XIth Int. Congr. Electron Microsc., Kyoto, pp. 963–964.

KOCH, F. B. & COHEN, J. B. (1969). *Acta Cryst.* B**25**, 275–287.

LEBRETON, C. & HOBBS, L. W. (1983). *Radiat. Eff.* **74**, 227–236.

VALLET, P. & CAREL, C. (1989). *Bull. Alloy Phase Diagrams*, **10**, 209–218.

Acta Cryst. (1991). B**47**, 337–344

Structures and Phase Transitions of $[(CH_3)_4As]_2CoCl_4$ and $[(CH_3)_4As]_2ZnCl_4$

BY F. J. ZÚÑIGA, M. J. CABEZUDO AND G. MADARIAGA

Departamento de Física de la Materia Condensada, Facultad de Ciencias, Universidad del País Vasco, Apdo 644, *Bilbao, Spain*

AND M. R. PRESSPRICH, M. R. BOND AND R. D. WILLETT

Department of Chemistry, Washington State University, Pullman, Washington 99165, *USA*

(*Received* 9 *July* 1990; *accepted* 26 *November* 1990)

Abstract

Two phase transitions of bis(tetramethylarsonium) tetrachlorocobaltate(II), $[(CH_3)_4As]_2CoCl_4$, and bis(tetramethylarsonium) tetrachlorozincate(II), $[(CH_3)_4As]_2ZnCl_4$, have been identified by calorimetry and X-ray diffraction. The compounds, isostructural with each other, have unusual tetragonal

0108-7681/91/030337-08$03.00